







Cite this: *RSC Adv.*, 2021, 11, 18342

Hydrogenated or oxyfunctionalized turpentine: options for automotive fuel components†

David Donoso, ^a Duban García, ^b Rosario Ballesteros, ^a Magín Lapuerta ^{*a} and Laureano Canoira ^c

Many concerns, such as economic and technical viability and social and ethical aspects, must be considered for a feedstock selection for advanced biofuels. Industrialized countries promote the use of industrial waste or by-products for this purpose. In particular, turpentine has several properties which make it an attractive source for biofuels, including its possible industrial waste origin. Nevertheless, turpentine has shown some disadvantages when blended directly with diesel, especially because it increases the sooting tendency. On the contrary, some derivatives of turpentine can be suitable for diesel blends. Thus, the evaluation of their properties is necessary. In the present work, the properties of hydrogenated and oxyfunctionalized turpentine have been analysed and compared with the purpose of elucidating their benefits and drawbacks in diesel fuel applications, using European standards as a reference. The results show a promising application of both hydroturpentine and oxyturpentine as diesel components. While hydroturpentine significantly improves the diesel cold flow properties, oxyturpentine noticeably reduces the sooting tendency.

Received 17th April 2021

Accepted 11th May 2021

DOI: 10.1039/d1ra03003e

rsc.li/rsc-advances

1. Introduction

Sustainable biofuels are an alternative to reduce the increasing global concentration of greenhouse gases (mainly CO₂), which are causing climate change. This renewable energy source can help solve this serious issue, especially if biofuels are autochthonous and have a residual origin. In Europe, Directive (EU) 2018/2001¹ identifies a series of advanced biofuels that mostly have these characteristics, targeting 3.5% of the final energy consumed by 2030 in the transport sector.

Turpentine, which can be obtained from different processes, is a mixture of terpenes, mainly monoterpenes (α - and β -pinene) and, in minor quantity, sesquiterpenes. Currently, turpentine is mainly obtained from the process of kraft softwood pulping as a by-product of the paper industry (in this case called crude sulfate turpentine) and by vacuum or steam distillation of oleoresin as a secondary product of resin industry (in this case named gum turpentine). Turpentine can also be obtained by solvent extraction of wood and dry distillation of aged pine stumps (in this case called wood turpentine), but these methods

are hardly ever used.² According to the aforementioned directive, crude sulfate turpentine can be considered an advanced biofuel since it derives from biomass fraction of industrial waste and does not interfere with the food or feed chain (Part A(d), Annex IX), whereas gum turpentine and wood turpentine can also be considered advanced biofuels since they derive from biomass fraction of wastes and residues from forestry and forest-based industries (Part A(o), Annex IX).

Among 316 kt of turpentine produced worldwide in 2019, ~60% was obtained from the paper industry and ~40% from pine resin. Only a minor portion was produced from stump wood (<2%).³ Currently, turpentine is commercialized with a market value of around 1.3 € per L and it is expected a decrease in this value with the increase in the participation of pine producers from other countries different to China, Brazil and USA. In the case of pine resin, for a productivity of 4 kg per pine per year, the cost of biofuel would be 0.54 € per kg, almost the same as the fossil diesel fuel. Increasing the productivity to 6 kg per pine per year would reduce the biofuel cost to 0.44 € per kg, lower than the price of fossil fuel.

Turpentine has been studied as a renewable fuel for transport sector (diesel,⁴⁻⁶ biodiesel,⁷ gasoline⁸ and jet fuels⁹). In particular, this renewable component can be suitable for heavy-duty diesel engines, which can hardly be replaced by electrification in the medium term. Despite turpentine has similar energy density to diesel fuel, unsaturated hydrocarbons and cyclic structure of the molecules makes turpentine inadequate as a diesel fuel component because of their high sooting tendency. Hence, some transformations have been proposed to overcome this negative effect, such as hydrogenation^{9,10} and

^aETS Ingeniería Industrial, Universidad de Castilla-La Mancha, Avda. Camilo José Cela s/n, 13071 Ciudad Real, Spain. E-mail: Magin.Lapuerta@uclm.es

^bEnvironmental Catalysis Research Group, School of Engineering, Chemical Engineering Department, Universidad de Antioquia, Calle 70 No. 52-21, Medellín, Colombia

^cDepartment of Energy & Fuels, ETS Ingenieros de Minas y Energía, Universidad Politécnica de Madrid, Ríos Rosas 21, 28003 Madrid, Spain

† Electronic supplementary information (ESI) available. See DOI: 10.1039/d1ra03003e



oxyfunctionalization,¹¹ among others.¹² These transformations have shown convincing effects on the properties of the fuels obtained. For instance, the oxyfunctionalized turpentine showed noticeable decrease in emissions of nitrogen oxides and particulate matter,¹³ in addition to its high suitability for diesel fuel applications due to its fuel properties,¹⁴ whereas hydrogenated turpentine possesses high fuel benefits such as high energy density, excellent cold flow properties and lower propensity to produce soot.⁹ However, a comparison of the fuels obtained from oxyfunctionalization and hydrogenation can help determine their suitability as automotive fuel components.

In this work, hydrogenated turpentine was separately blended with diesel and biodiesel. Both sets of blends were subjected to measurements of the main fuel properties. The results were compared with those obtained in a previous work¹⁴ for the same blends with oxyturpentine and raw turpentine. All results were evaluated using the European standard for diesel fuels as a reference, to investigate the influence of the hydrogenation reaction in the fuel properties and assessing the potential of hydroturpentine as a diesel fuel component. At the same time, hydroturpentine and oxyturpentine were compared, looking for benefits and drawbacks of both turpentine-derived fuels.

2. Materials and methods

2.1. Fuels

Turpentine was supplied by Resinas Naturales SL (Cuéllar, Spain). Hydroturpentine and oxyturpentine were produced as described in previous works.^{9,11} Briefly, on the one hand, batches of 136 g of turpentine were hydrogenated with absolute ethanol as solvent (100 mL) and 1% Pt/Al₂O₃ as catalyst (3% w/w respect to turpentine), using a low-pressure autoclave. The reaction conditions were: 60 °C, 6 bar H₂, 300 rpm, and 4.5 h. On the other hand, batches of 143 g of turpentine were oxyfunctionalized with paraformaldehyde (in equimolar ratio) as reagent and Sn-MCM-41 as catalyst (8% w/w respect to turpentine) in a flask equipped with a reflux condenser and temperature control. The reaction conditions were: 90 °C, atmospheric pressure, 1000 rpm, and 24 h. Conversion was calculated using eqn (1), where C_i and C_f are the initial and final concentrations, respectively, of both pinenes (α - and β -pinene).

$$\text{Conversion(\%)} = \frac{C_i(\text{pinenes}) - C_f(\text{pinenes})}{C_i(\text{pinenes})} \quad (1)$$

Both hydrogenation and oxyfunctionalization showed moderate conversions (34% and 42%, respectively) because reaction conditions favoured the conversion of β -pinene to pinane and to nopol, respectively. In the former case, the endocyclic double bond of α -pinene was difficult to hydrogenate because such bond is less accessible than the exocyclic double bond present in β -pinene. In the latter case, the conversion of α -pinene to α -terpineol was low because the catalyst used in the oxyfunctionalization reaction was selected to maximize the conversion of β -pinene.

Diesel was supplied by Repsol (Spain) as first fill diesel, *i.e.*, without any oxygenated component, whereas biodiesel was supplied by BioOils Energy (Spain) and was produced from a mixture of soybean and palm oils.

2.2. Fuel characterization

Density was measured based on standard EN ISO 3675, using a 10 mL glass pycnometer and a climatic chamber Ineltec (used to soak the sample at 15 °C and 45% relative humidity).

Kinematic viscosity was measured using a Froton viscosimeter 75 series and a Tamson thermostatic visibility bath (model: TV 2000) to keep the sample at 40 °C, following standard EN ISO 3104.

Lubricity was measured with a High Frequency Reciprocating Rig (HFRR) from PCS Instruments, based on standard EN ISO 12156-1. Wear Scar Diameter (WSD) was measured using a stereomicroscope Optika SZ-CTV coupled to Motical 2500 digital camera (equipped with 100× magnification lens). All tests were made inside a climatic chamber from PCS Instruments where the ambient temperature and humidity were controlled with the use of salts. Repeatability was proved to be lower than 20 μm ,¹⁵ which is below that required in the European standard (max. repeatability: 50 μm).

Higher heating value (HHV) was measured in a calorimetric bomb Parr 1351 (USA) following standard UNE 51123. The lower heating value (LHV) was calculated from the measured HHV and the elemental composition of sample through eqn (2) (where Y_H and Y_O are the mass fractions of hydrogen and oxygen in the fuel, respectively), *i.e.*, subtracting the heat of vaporization of water in the combustion products from the HHV.

$$\text{LHV} = \text{HHV} - 21.365 Y_H - 0.077 Y_O \quad (2)$$

Derived Cetane Number (DCN) was measured in a Cetane Ignition Delay 510 from PAC instruments following standard EN 16715.

Flash point was measured in an automated Pensky–Martens Closed Cup Flash Point Tester SETA PM-93, following standard EN ISO 2719.

Regarding cold flow properties, cloud point and pour point were measured following standards EN 23015 and EN ISO 3016, respectively. The cold flow behaviour was also studied by Differential Scanning Calorimetry (DSC). The Crystallisation Onset Temperature (COT) was determined as the temperature at which the heat release from crystallisation starts, using a Q20 TA DSC Instrument, as it was done in a previous study.⁹

Smoke point was measured in a standardized lamp following standard ASTM D1322. Three calibration blends of isooctane and toluene were prepared, with 10, 20 and 30% v/v of toluene. To compare the sooting tendency between fuels, Oxygen Extended Sooting Index (OESI) was calculated as proposed by Barrientos *et al.*¹⁶ for diffusion flames (after estimating the molecular weights of the blends as shown in the ESI†), under a 0–100 scale with 0 corresponding to isooctane and 100 to toluene. In previous works,^{14,17} constants a' (43.588 mm⁻¹) and b' (−5.7177) were obtained from calibration with isooctane and toluene under the same experimental conditions (burner and laboratory).

2.3. Experimental matrix

In a previous work,¹⁴ turpentine and oxyturpentine were blended separately with diesel and biodiesel fuels in contents 1%, 2%, 3%, 5%, 10%, 15% and 20% v/v. Fuel characterisation (density, kinematic viscosity, lubricity, heating values, derived



cetane number, flash point, smoke point, sooting tendency, cloud point, pour point, and crystallization temperature) was performed for these blends. To compare, hydroturpentine was blended with diesel and biodiesel fuels in the same contents. The mean molecular formula, molecular weight, H/C ratio and fuel/air stoichiometric ratio of pure fuels are shown in Table 1S of the ESI.† The same fuel characterisation was made for pure fuels (Table 2S†), for diesel blends (Table 3S†), and for biodiesel blends (Table 4S†). Contents beyond 20% v/v were discarded because some properties such as derived cetane number were expected to be deteriorated notably. Low contents were analysed trying to look for synergistic effects. The limits in properties established in standards EN 590 and EN 14214 for European diesel and biodiesel fuels, respectively, were used to compare the properties of the six groups of blends (hydroturpentine, oxyturpentine and turpentine with diesel and biodiesel fuels). The range between limits is shadowed in the following figures. Therefore, the potential of hydroturpentine and oxyturpentine as fuel components were assessed and compared.

3. Results and discussion

3.1. Composition

The composition of turpentine, hydroturpentine and oxyturpentine (denoted as T, HT, and OT, respectively) was analysed by GC-MS and the main components are shown in Table 1. As can be observed, the most of β -pinene content in turpentine was transformed into pinane (in case of hydroturpentine) and nopol (in case of oxyturpentine).

3.2. Physical properties

Density of hydroturpentine, oxyturpentine and turpentine blends with diesel and biodiesel is shown in Fig. 1. The hydrogenation process slightly reduces the density of turpentine,

whereas the oxyfunctionalization reaction of turpentine significantly increases its density. Since diesel has a lower density, hydroturpentine needs to be blended to fulfil the limits established in standard EN 590 with the same blending ratio as for turpentine (around 50% v/v). In contrast, only around 20% v/v of oxyturpentine can be blended with diesel fuel to remain between limits. However, it must be remarked that the diesel fuel used in this work (first-fill diesel) has a relatively low density with respect to the usual commercial diesel fuel (with presence of biodiesel) and therefore, blending ratios should be slightly lower. In case of blends with biodiesel, hydroturpentine shows lower density, remaining between the limits established in standard EN 14214, whereas oxyturpentine blends are out of range beyond 60% v/v.

As observed in Fig. 2, contrary to turpentine blends, excess volumes become significant for both hydroturpentine and oxyturpentine blends, especially for the former ones. However, these excess volumes have opposite sign for diesel blends (negative) and for biodiesel blends (positive). This can be explained by the better molecular packaging between diesel molecules (with a diversity of cyclic and linear structures) and terpenic molecules (mostly cyclic) in diesel blends, and worse molecular packaging between ester molecules (linear structures) and terpenic ones in biodiesel blends.

Viscosity of hydroturpentine, oxyturpentine and turpentine blends with diesel and biodiesel is shown in Fig. 3. Both hydrogenation and oxyfunctionalization increase viscosity. However, such increase is only slight for hydrogenation but very significant for oxyfunctionalization. The three terpenic biofuels

Table 1 Chemical composition (% w/w) of turpentine, hydroturpentine and oxyturpentine^a

Compound	T	HT	OT
α -Pinene	67.3	56.8	47.1
β -Pinene	21.5	2.2	4.2
Pinane (<i>endo</i> or <i>exo</i>)	n.d.	27.3	n.d.
Nopol	n.d.	n.d.	31.7
α -Terpineol	0.3	n.d.	4.7
D-Limonene	2.7	0.3	0.6
1- <i>p</i> -Menthene	n.d.	2.8	n.d.
<i>p</i> -Menthane	n.d.	0.6	n.d.
3-Carene	n.d.	n.d.	2.1
Caryophyllene	2.2	n.d.	n.d.
Longifolene	2.0	3.6	0.1
Camphene	1.2	n.d.	1.3
Myrcene	1.0	n.d.	1.3
α -Phellandrene	n.d.	n.d.	1.6
α -Longipinene	0.2	0.3	1.1
(+)-Fenchone	n.d.	n.d.	1.1
Isoborneol	n.d.	n.d.	0.7
Others	1.6	6.1	2.4

^a n.d. = not detected.

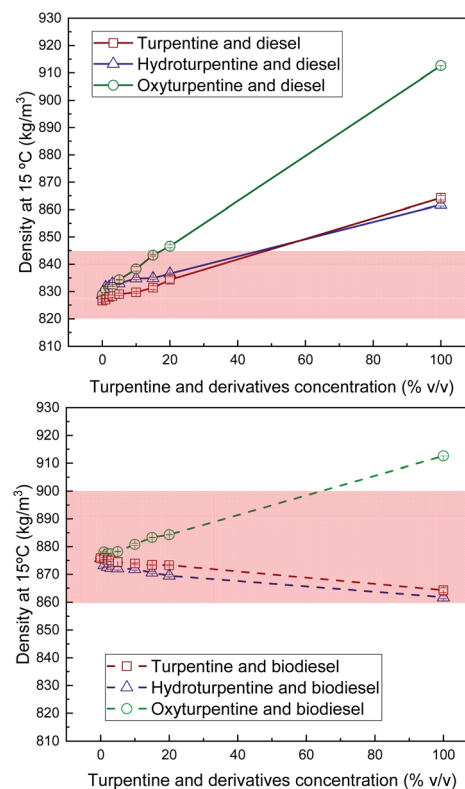


Fig. 1 Density of diesel blends with T, HT, and OT (top), and of biodiesel blends with T, HT, and OT (bottom).

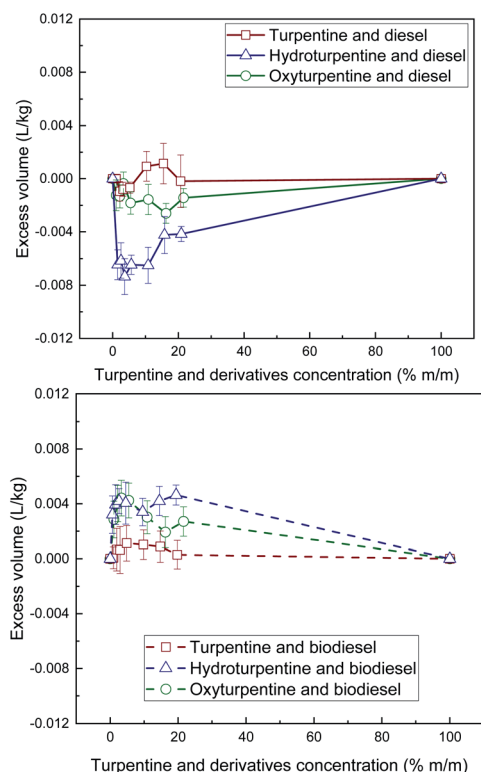


Fig. 2 Excess volume of diesel blends with T, HT, and OT (top), and of biodiesel blends with T, HT, and OT (bottom).

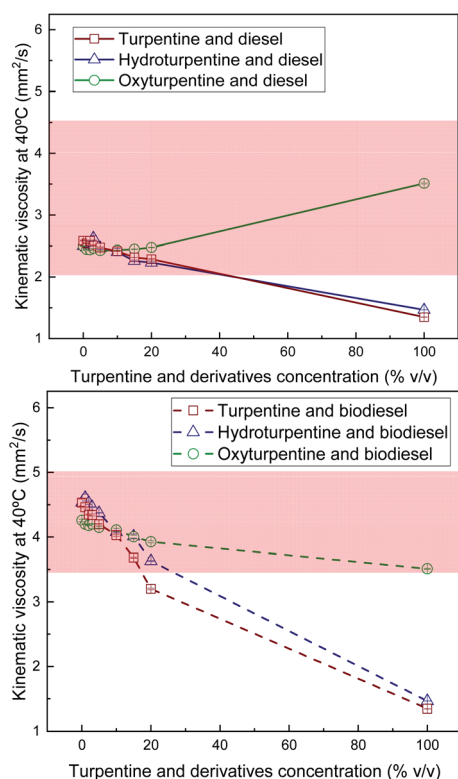


Fig. 3 Kinematic viscosity of diesel blends with T, HT, and OT (top), and of biodiesel blends with T, HT, and OT (bottom).

Table 2 Grunberg–Nissan coefficients of turpentine, hydroturpentine and oxyturpentine blends with diesel and biodiesel

	T	HT	OT
Diesel	0.230	−0.104	−0.605
Biodiesel	0.454	0.707	−0.100

show lower viscosity than biodiesel, while only turpentine and hydroturpentine present lower viscosity than diesel. Hydroturpentine–diesel blends show similar trend as turpentine–diesel blends. The blending limit would be 40% v/v of terpenic biofuel. On the contrary, all oxyturpentine–diesel blends remain between limits established in standard EN 590. Hydroturpentine–biodiesel blends could extend the limit concentration with respect to turpentine–biodiesel blends from less than 20% to around 25% v/v. Oxyturpentine–biodiesel blends fulfil the limits required in standard EN 14214 for any concentration, although viscosity of oxyturpentine gets close to the lower limit.

Since all blends show non-linear trends for viscosity with respect to composition, Grunberg–Nissan correlation¹⁸ was applied (eqn (3)), and the interaction coefficient (G) was determined by fitting to the experimental values.

$$\ln(\rho\nu) = x_1 \ln(\rho_1\nu_1) + x_2 \ln(\rho_2\nu_2) + x_1x_2G \quad (3)$$

where x represents the molar fraction, ν and ρ are the kinematic viscosity and the density of the blend, respectively, and subscripts 1 and 2 represent the components of binary blend. The interaction coefficients of Grunberg–Nissan obtained for the blends of turpentine, hydroturpentine and oxyturpentine with diesel and biodiesel are summarized in Table 2. These coefficients are consistent with those obtained in alcohol blends, which are always lower when alcohols are blended with diesel than when they are blended with biodiesel.¹⁹

Lubricity of hydroturpentine, oxyturpentine and turpentine blends with diesel and biodiesel is shown in Fig. 4.

Hydroturpentine and oxyturpentine improve the lubricity of turpentine and both show lower WSD values than the maximum limit established in standard EN 590, thus guaranteeing a good performance and durability of the engine. Hydroturpentine shows worse lubricity than oxyturpentine. A significant positive synergistic effect can be observed in all diesel blends and in hydroturpentine–biodiesel blends for low concentrations of terpenic biofuel, similarly as those observed with different biodiesel–diesel blends (*e.g.*, palm oil biodiesel,²⁰ soybean oil biodiesel,²¹ castor oil biodiesel).²² Then, friction and/or wear can be reduced with the use of these terpenic biofuels in low concentrations of terpenic biofuel.

3.3. Combustion and thermochemical properties

LHV values were calculated from the measured HHV and the elemental composition and are shown in Fig. 5 (per unit mass) and Fig. 6 (per unit volume). Although hydroturpentine increases HHV significantly with respect to turpentine, LHV (per unit mass) is only slightly higher because the increase in



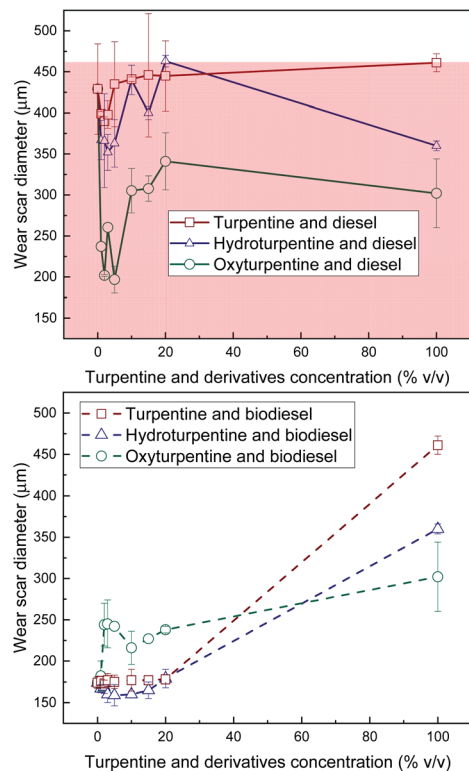


Fig. 4 WSD of diesel blends with T, HT, and OT (top), and of biodiesel blends with T, HT, and OT (bottom).

hydrogen content is almost compensated by the higher water content in the combustion products (and thus higher difference HHV–LHV). When LHV is expressed per unit volume,

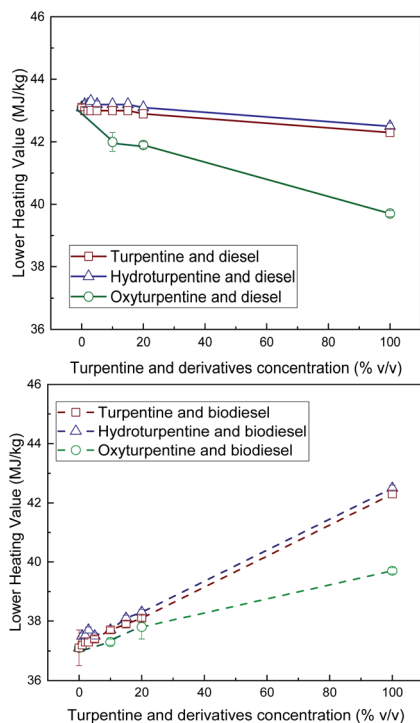


Fig. 5 LHV (per unit mass) of diesel blends with T, HT, and OT (top), and of biodiesel blends with T, HT, and OT (bottom).

hydroturpentine remains unchanged with respect to turpentine. On the contrary, oxyturpentine shows lower HHV and LHV than turpentine both in mass and volume basis. However, both hydroturpentine (similarly to turpentine) and oxyturpentine show higher LHV than diesel (in volume basis) and biodiesel (in mass and volume basis). Hydroturpentine–diesel blends show a positive synergistic effect in all concentration levels, this effect being more significant for LHV per unit volume. Hydroturpentine–biodiesel blends also show a positive synergistic effect but only for very low concentration levels. On the other hand, oxyturpentine–diesel blends show lower LHV (in both mass and volume basis) than hydro- and turpentine diesel blends, showing an antisnergistic effect in case of LHV (in volume basis). Oxyturpentine blends with biodiesel show a linear trend for LHV in both mass and volume basis. The same linear trend is observed for turpentine blends in all cases.

Flash point of turpentine, hydroturpentine, and oxyturpentine blends with diesel and biodiesel is shown in Fig. 7. Hydrogenation increases turpentine inflammability due to the presence of more volatile compounds (*e.g.*, pinane) whereas oxyfunctionalization barely modifies this property. However, both biofuels (specially oxyturpentine) improve flash point in blends with diesel and biodiesel compared to blends of turpentine with these reference fuels. Blends of hydroturpentine and oxyturpentine could be blended with diesel up to 20% and around 40% v/v (see Fig. 7, top), respectively, fulfilling minimum limit (55 °C) established in standard EN 590, thus guaranteeing safety related to fire hazard.²³ However, only

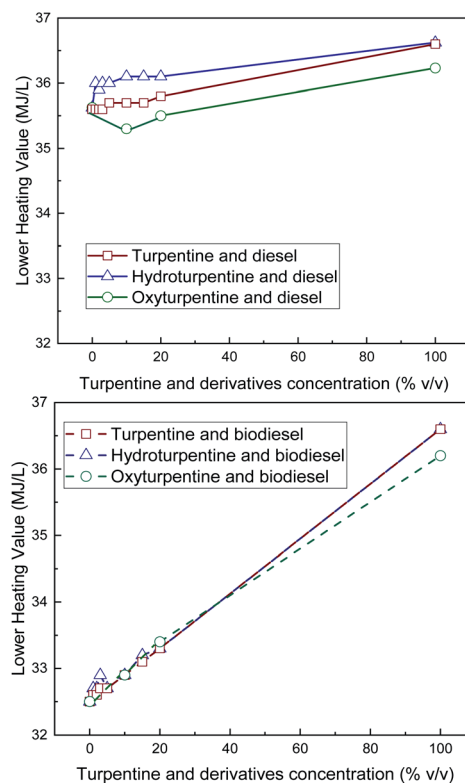


Fig. 6 LHV (per unit volume) of diesel blends with T, HT, and OT (top), and of biodiesel blends with T, HT, and OT (bottom).



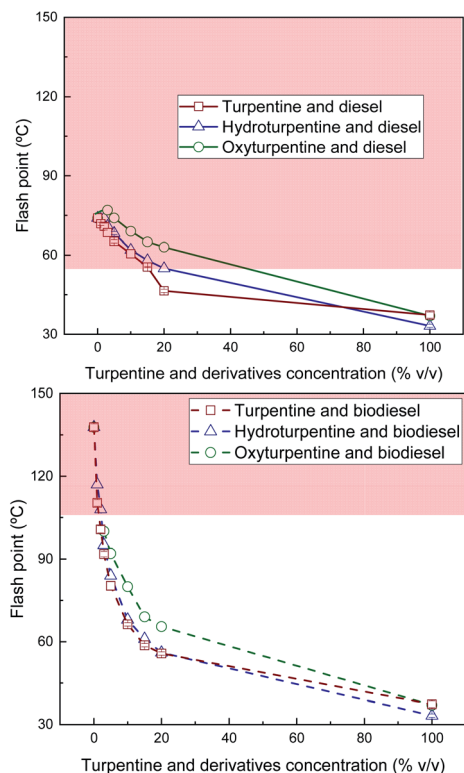


Fig. 7 Flash point of diesel blends with T, HT, and OT (top), and of biodiesel blends with T, HT, and OT (bottom).

very low blend-concentrations of these biofuels with biodiesel show a flash point higher than the minimum limit (101 °C) established in standard EN 14214 (see Fig. 7, bottom). This implies that modifications in the biodiesel standard would be required before commercialization of blends with higher terpene concentration.

Derived cetane number of turpentine, hydroturpentine, and oxyturpentine blends with diesel and biodiesel is shown in Fig. 8. Hydrogenation improves this property with respect to that of turpentine, whereas oxyfunctionalization does not affect it. However, the derived cetane number of these pure biofuels is far below the minimum limit (51) established in standards EN 590 and EN 14214. Consequently, DCN decreases with increasing concentration for all hydro-, oxy- and turpentine blends (with both diesel and biodiesel fuels). Such decrease is almost linear in turpentine blends with diesel and biodiesel and oxyturpentine–biodiesel blends. However, some synergistic effect is observed in all other diesel and biodiesel blends. Oxyturpentine–diesel blends show a positive synergistic effect in low concentrations (up to 10% v/v), while hydroturpentine–diesel blends show an anti-synergistic effect. On the contrary, hydroturpentine–biodiesel blends show a positive synergistic effect in low concentrations (up to 15% v/v). Hydroturpentine–diesel blends show lower DCN than turpentine–diesel blends, despite hydroturpentine shows better DCN than turpentine. In fact, hydroturpentine–diesel blends would need some cetane enhancer additive to reach the minimum limit (51) in blends from 2% v/v. On the contrary, diesel blends with up to 25% v/v

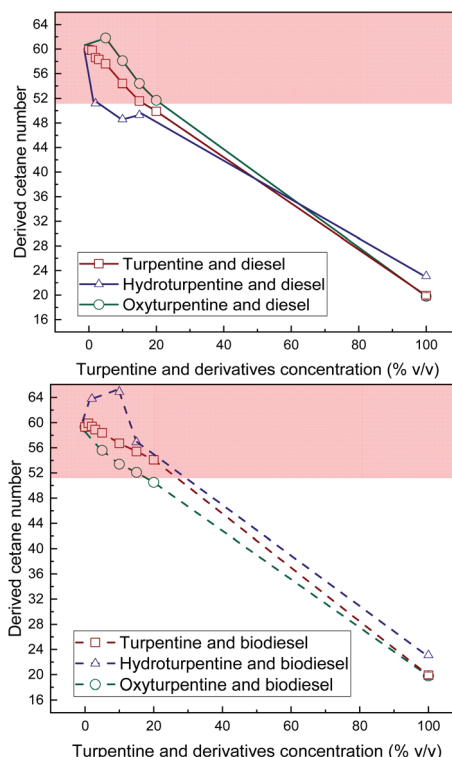


Fig. 8 Derived cetane number of diesel blends with T, HT, and OT (top), and of biodiesel blends with T, HT, and OT (bottom).

of oxyturpentine fulfil the minimum limit without any need of additives. Opposite effect is found for biodiesel blends. Considering these results, hydroturpentine could be blended up to 30% v/v with biodiesel and up to 20% v/v of oxyturpentine with this reference fuel fulfilling the limit.

Sooting tendency of fuels is inversely proportional to their smoke point. This inverse relation has been quantified with different parameters, such as TSI for hydrocarbons²⁴ and OESI for oxygenated hydrocarbons.^{16,17} Since both hydrocarbons and oxygenates are used in this study, OESI was selected as a common basis for comparison. Smoke point and OESI of hydroturpentine, oxyturpentine and turpentine blends with diesel are shown in Fig. 9 (top) and Fig. 9 (bottom), respectively. It was not possible to measure the smoke point for biodiesel blends due to excessive viscosity.²⁵ The hydrogenation process improves slightly the smoke point of turpentine whereas oxyfunctionalization greatly increases this property, as shown in Fig. 9 (top). Aromatization of the six-membered rings of the α -pinene and β -pinene in the first step of the combustion process could explain that turpentine shows lower smoke point than hydro- and oxyturpentine.²⁶

Among diesel blends, both hydro- and oxyturpentine blends (specially the latter ones) show better smoke point than turpentine blends. Fig. 9 (bottom) confirms the decrease in sooting tendency with both hydrogenation and oxyfunctionalization. Both hydro- and oxyturpentine blends show lower OESI than turpentine–diesel blends. Blends up to 10% v/v hydroturpentine show similar OESI than diesel and all



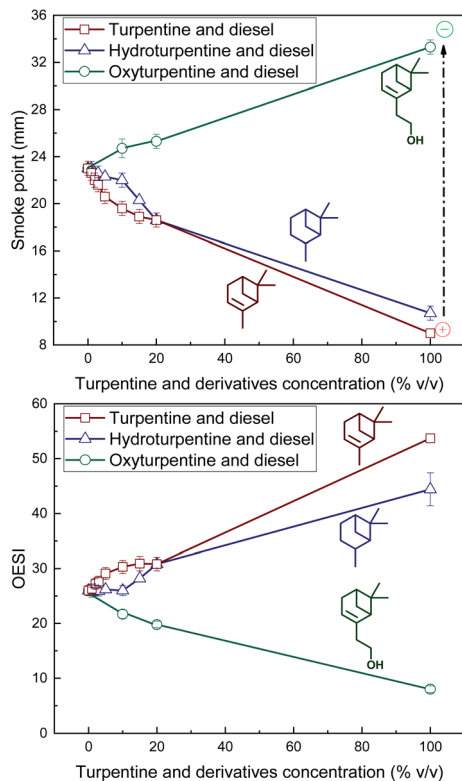


Fig. 9 Smoke point (top) and OESI (bottom) of diesel blends with T, HT, and OT.

oxyturpentine–diesel blends show lower OESI than pure diesel. Therefore, OESI demonstrates that the benefit in sooting tendency of both hydrogenation and oxyfunctionalization is more evident than that shown by smoke point results, because molecular weight is considered.¹⁶

3.4. Cold flow properties

Cloud and pour points and Crystallisation Onset Temperature (COT) were measured on turpentine, hydroturpentine and oxyturpentine blends with diesel and biodiesel fuels to evaluate their cold flow behaviour. Results are shown in Fig. 10–12, respectively. These properties can help identify the temperatures at which the fuel delivery could cause operational problems. It was not possible to obtain these cold flow properties for hydroturpentine, and only pour point was obtained for oxyturpentine. However, COT can be considered lower than -90°C for any terpenic biofuel since no exothermic peak appears in thermograms. Since oxyturpentine shows a pour point 6.9°C higher than that of turpentine, oxyfunctionalization is expected to deteriorate cold flow properties of turpentine. Hydroturpentine–diesel blends show lower cold flow properties than turpentine–diesel blends, whereas hydroturpentine–biodiesel blends have similar cold flow properties than turpentine–biodiesel blends except COT, which is better for hydroturpentine–biodiesel blends.

On the other hand, oxyturpentine–diesel blends show worse cold flow behaviour than turpentine–diesel blends, whereas no

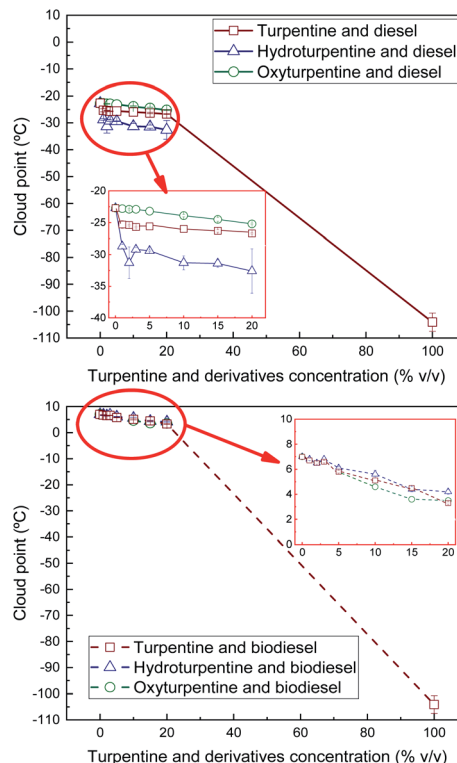


Fig. 10 Cloud point of diesel blends with T, HT, and OT (top), and of biodiesel blends with T, HT, and OT (bottom).

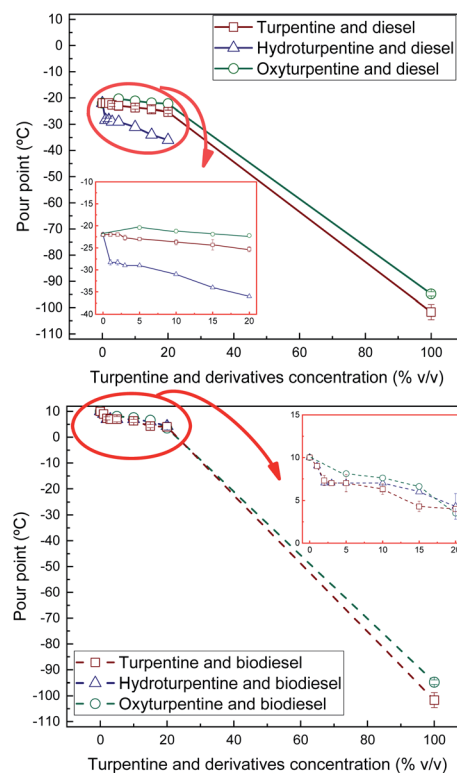


Fig. 11 Pour point of diesel blends with T, HT, and OT (top), and of biodiesel blends with T, HT, and OT (bottom).



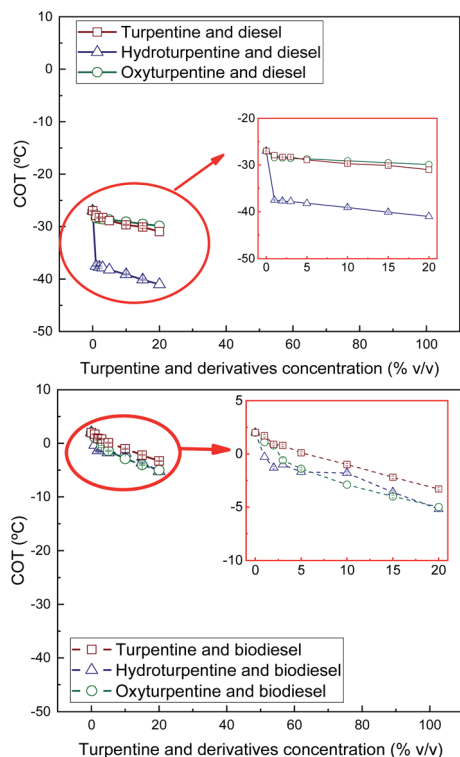


Fig. 12 COT of diesel blends with T, HT, and OT (top), and of biodiesel blends with T, HT, and OT (bottom).

clear trend is observed when comparing oxy- and turpentine blends with biodiesel.

In summary, the presence of a terpenic biofuel (either turpentine, hydroturpentine or oxyturpentine) significantly improves the cold flow properties of both reference fuels (diesel and biodiesel). These trends have already been observed in other works.^{9,27} Specifically, the sharp improvement in cold flow properties (reductions between 6–11 °C) observed in diesel blends with low hydroturpentine contents (1% v/v, *i.e.*, 10 000 ppm) suggests that hydroturpentine would be a competitive cold flow depressant for diesel fuel, with similar performance as some commercial depressors.²⁸

4. Conclusions

Turpentine has been proven as a suitable diesel component, since it mostly has an industrial waste origin, and very good properties, such as heating value and cold flow behaviour. On the contrary, its high sooting tendency is a practical barrier for its use in automotive diesel engines. However, this property can be improved, without negatively affecting other properties, when turpentine is subjected either to hydrogenation or to oxyfunctionalization. Both hydro- and oxyturpentine improve density, viscosity, lubricity, flash point and derived cetane number with respect to turpentine. Such improvements lead direct blends of these biofuels up to 20% v/v to fulfill the diesel standard limits. However, hydroturpentine–diesel blends would need cetane improvers to comply with the standard limit.

Heating values (in both mass and volume basis) are improved in hydroturpentine blends, contrarily to oxyturpentine blends. With regard to cold flow properties, hydroturpentine blends show better behaviour than turpentine blends and even better than oxyturpentine blends. Sooting tendency is significantly improved in oxyturpentine blends, while hydroturpentine blends slightly improve this property. Therefore, both hydroturpentine and oxyturpentine can be used in diesel applications. Hydroturpentine would be especially appropriate as diesel component in cold countries whereas oxyturpentine would be helpful in almost-zero emission developments.

Author contributions

D. Donoso: investigation, data curation, writing-original draft, D. García: investigation, formal analysis, data curation, R. Ballesteros: formal analysis, supervision, M. Lapuerta: conceptualization, writing-review & editing, project administration, L. Canoira: conceptualization, resources, supervision.

Conflicts of interest

There are no conflicts to declare.

Acknowledgements

Financial support by Junta de Comunidades de Castilla-La Mancha (Project FUELCAM, SBPLY/17/180501/000299) is gratefully acknowledged. David Donoso acknowledges University of Castilla-La Mancha (UCLM) for the predoctoral contract (Ref. 2019-PREDUCLM-10887). The authors also wish to thank the graduate students José A. Tébar, Sergio Rodríguez and Jesús Abad (UCLM) for their technical contribution to this work and the company Resinas Naturales SL (Cuéllar, Spain) for the generous donation of materials.

References

- 1 Directive (EU) 2018/2001 of the European Parliament and of the Council of 11 December 2018 on the promotion of the use of energy from renewable sources, 2018.
- 2 M. Gscheidmeier and H. Fleig, Turpentine, in *Ullman's Encyclopedia of Industrial Chemistry*, ed. B. Elvers and S. Hawkins, VCH Publishers, New York, 1996, pp. 267–280.
- 3 Ultra International B.V., *Terpenes. A major renewable and sustainable source of fragrance and flavour ingredients*, 2019, <http://ultranl.com/terpenes/>, last accessed, April 16, 2021.
- 4 N. I. Tracy, D. Chen, D. W. Crunkleton and G. L. Price, *Fuel*, 2009, **88**, 2238–2240.
- 5 R. Karthikeyan and N. Mahalakshmi, *Energy*, 2007, **32**, 1202–1209.
- 6 B. P. Anand, C. G. Saravanan and C. A. Srinivasan, *Renewable Energy*, 2010, **35**, 1179–1184.
- 7 P. Dubey and R. Gupta, *Renewable Energy*, 2018, **15**, 1294–1302.
- 8 O. Arpa, R. Yumrutas and M. H. Alma, *Energy*, 2010, **35**, 3603–3613.



- 9 D. Donoso, R. Ballesteros, D. Bolonio, M. J. García-Martínez, M. Lapuerta and L. Canoira, *Energy Fuels*, 2020, **35**, 1465–1475.
- 10 S. Hou, X. Wang, C. Huang, C. Xie and S. Yu, *Catal. Lett.*, 2016, **146**, 580–586.
- 11 D. García, F. Bustamante, A. L. Villa, M. Lapuerta and E. Alarcón, *Energy Fuels*, 2020, **34**, 579–586.
- 12 J. K. Jung, Y. Lee, J. W. Choi, J. Jae, J. M. Ha, D. J. Suh, *et al.*, *Energy Convers. Manag.*, 2016, **116**, 72–79.
- 13 D. García, Á. Ramos, J. Rodríguez-Fernández, F. Bustamante, E. Alarcón and M. Lapuerta, *Energy*, 2020, **201**, 117645.
- 14 R. Ballesteros, D. García, F. Bustamante, E. Alarcón and M. Lapuerta, *Renewable Energy*, 2020, **162**, 2210–2219.
- 15 M. Lapuerta, J. Sánchez-Valdepeñas, D. Bolonio and E. Sukjit, *Fuel*, 2016, **184**, 202–210.
- 16 E. J. Barrientos, M. Lapuerta and A. L. Boehman, *Combust. Flame*, 2013, **160**, 1484–1498.
- 17 A. Llamas, M. Lapuerta, A. M. Al-Lal and L. Canoira, *Energy Fuels*, 2013, **27**, 6815–6822.
- 18 L. Grunberg and A. H. Nissan, *Nature*, 1949, **164**, 799–800.
- 19 M. Lapuerta, J. Rodríguez-Fernández, D. Fernández-Rodríguez and R. Patiño-Camino, *Fuel*, 2017, **199**, 332–338.
- 20 M. A. Mujtaba, H. M. Cho, H. H. Masjuki, M. A. Kalam, M. Farooq, M. E. M. Soudagar, *et al.*, *Energy Rep.*, 2020, **7**, 1162–1171.
- 21 M. M. Maru, R. M. Trommer, K. F. Cavalcanti, E. S. Figueiredo, R. F. Silva and C. A. Achete, *Energy*, 2014, **69**, 673–681.
- 22 L. Canoira, J. García-Galeán, R. Alcántara, M. Lapuerta and R. García-Contreras, *Renewable Energy*, 2010, **35**, 208–217.
- 23 J. A. Lazzús, *Chin. J. Chem. Eng.*, 2010, **18**, 817–823.
- 24 H. F. Calcote and D. M. Manos, *Combust. Flame*, 1983, **49**, 289–304.
- 25 O. Armas, M. A. Gómez, E. J. Barrientos and A. L. Boehman, *Energy Fuels*, 2011, **25**, 3283–3288.
- 26 L. H. Duong, I. K. Reksowardojo, T. H. Soerawidjaja, D. N. Pham and O. Fujita, *Combust. Sci. Technol.*, 2018, **190**, 1710–1721.
- 27 J. K. Kumar, C. S. Raj, P. Gopal and P. S. Kumar, *Int. J. Chem. Sci.*, 2016, **14**, 1307–1316.
- 28 T. Yang, S. Yin, M. Xie, F. Chen, B. Su, H. Lin, *et al.*, *Fuel*, 2020, **272**, 117666.

